Throughput Analysis for a UMTS High Speed Downlink Packet Access LMMSE Equalizer

K. Freudenthaler[1], F. Kaltenberger[2], S. Geirhofer[3], S. Paul[4], J. Berkmann[4], J. Wehinger[5], C.F. Mecklenbräuker[5], A. Springer[1]

[1] Institute for Communications and Information Engineering, University of Linz, Austria, k.freudenthaler@icie.jku.at
[2] ARC Seibersdorf Research GmbH, Donau-City Str. 1, A-1220 Wien, Austria, florian.kaltenberger@arcs.ac.at
[3] Institute of Communications and Radio-Frequency Engineering, Vienna University of Technology, Austria, sgeirhof@nt.tuwien.ac.at
[4] Infineon Technologies AG, Secure Mobile Solutions D-81609 München, Germany, {steffen.paul,jens.berkmann}@infineon.com
[5] ftw. Forschungszentrum Telekommunikation Wien, A-1220 Wien, Austria, {wehinger,cfm}@ftw.at

***Abstract*— UMTS addresses future packet services over channels with fluctuating quality via its High Speed Downlink Packet Access (HSDPA) sub-system. The throughput over HSDPA decreases significantly due to Multiple Access Interference (MAI). In this contribution, it is shown by simulation that the Linear Minimum Mean Square Error (LMMSE) equalizer shows superior throughput than a conventional RAKE receiver. The gain in E_c/I_{or} is approximately 1.6–2 dB depending on the modulation scheme.**

We have developed a simulation environment specifically tailored to HSDPA for investigating the HSDPA receiver requirements. The downlink physical layer for the user data on the High Speed Physical Downlink Shared Channel (HS-PDSCH) is modelled in detail, whereas the associated signalling is idealised as error-free. The interference from signalling and data channels on the HS-PDSCH is modelled adequately. As a general guideline for system settings in the simulations, we use the test cases specified in 3GPP TS 25.101 whenever applicable.

I. Introduction

UMTS features moderately high data rates for packet data services [1], [2], [3]. Efficient, fast, and flexible assignment of radio resources to packet users is highly desirable from both a user's and an operator's viewpoint. UMTS addresses future packet services over channels with fluctuating channel quality via its HSDPA sub-system. We have developed a simulation environment specifically tailored to HSDPA for investigating the HSDPA receiver requirements [6]. Particular care was devoted to adequate modelling of interference on the HS-PDSCH.

MAI as well as the interference from signalling channels like SCH and CPICH significantly degrade the performance of a HSDPA system, when a RAKE receiver is used. Recently [7], we have investigated throughput enhancements by cancellation of SCH and CPICH. In the case of an AWGN channel an improvement of 1 dB was achieved whereas in the case of a frequency selective channel, no significant improvement was found. In this paper, we investigate the throughput performance of an HSDPA receiver employing a LMMSE equalizer [8].

Similar investigations were carried out in [9], however no uplink channel for signalling either positive or negative acknowledgements (ACK/NACK) was implemented and hence not the full functionality of the Hybrid Automatic Repeat ReQuest (HARQ) was exploited.

The paper proceeds with a description of the HSDPA subsystem. In Sec. 3 and 4 respectively the simulator and the receiver architecture are documented. In Sec. 5, results on throughput performance from the numerical experiments over the frequency selective channels International Telecommunication Union (ITU) Pedestrian-B and Vehicular-A [5] are presented. The paper concludes with a discussion of the results.

II. HSDPA System Description

HSDPA introduces three physical channels into UMTS Release 5. The HS-PDSCH is the data channel which is shared by all HSDPA users of a single cell in the time and code domain. The HS-PDSCH consists of up to 15 subchannels corresponding to 15 Walsh-Hadamard channelization codes with Spreading Factor (SF) 16. The Transmission Time Interval (TTI) is 2 ms, which is called a subframe. A fast scheduler which resides in the Node-B is responsible for selecting packets to be transmitted in each subframe [6]. Up to four High Speed Shared Control Channels (HS-SCCH) inform the selected users on the used Modulation and Coding Scheme (MCS), the current HARQ process, and the Redundancy and Constellation Version (RV) of the retransmission. An uplink signalling channel, the so-called High Speed Dedicated Physical Control Channel (HS-DPCCH), is assigned to each HSDPA user. The HS-DPCCH carries ACKs, respectively NACKs, as well as the Channel Quality Indicator (CQI). The ACK/NACK and the CQI are transmitted no later than 7.5 slots after the corresponding subframe was transmitted.

Three closely coupled procedures govern the performance of the HSDPA, namely: Adaptive Modulation and Coding (AMC), fast HARQ, and fast packet scheduling [10].

A. Adaptive Modulation and Coding

Instead of compensating the varying downlink radio conditions on the HS-PDSCH by means of fast power control at a fixed data rate, the data rate is adjusted depending on measured channel quality in each subframe. The data rate adjustment is achieved by puncturing and repetition ("rate matching") of the

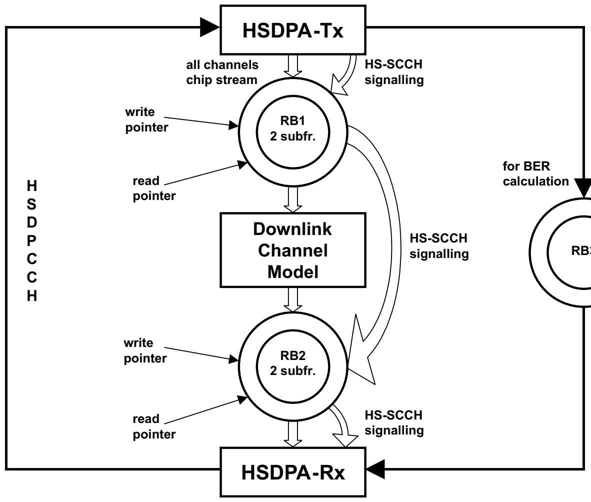

Fig. 1. HSDPA Simulator architecture with three ringbuffers (RB).

rate $1/3$ turbo-coded data stream and by selecting either QPSK modulation or 16QAM [6].

B. Fast HARQ

In HSDPA, it is foreseen that the User Equipment (UE) stores the data from previous transmissions to enable joint decoding of retransmissions with incremental redundancy (IR). The IR versions are generated by rate matching and constellation rearrangement in case of 16QAM. The UE needs internal memory to store the original data packet which is combined with the retransmitted packet. This technique increases the probability of successful decoding for retransmissions significantly. Retransmissions are requested until the data are correctly decoded or a maximum number of attempts is exceeded [6].

C. Fast Scheduling

A key component of HSDPA is the packet scheduler, which is located in the Node-B. For each TTI the scheduling algorithm controls the allocation of channelization codes on the HS-PDSCH to the users. The scheduling policy itself is not standardized in UMTS. Various trade-offs between simplicity, total throughput, and user fairness can be implemented [6].

III. Simulator Description

The HSDPA link-level baseband simulator is implemented in the MATLAB language. The simulator consists of the Node-B transmit side, the downlink channel model, the HSDPA receiver, and three ringbuffers (RB), as illustrated in Fig. 1. The simulator is modular such that implementation of the transmitter, the channel, and the receiver can easily be changed by other implementations [6].

For each subframe the HSDPA transmitter generates the HS-PDSCHs for the scheduled users, the SCH, the Primary Common Control Physical Channel (P-CCPCH) and the Primary-CPICH (P-CPICH) according to [2]. In our current implementation the Paging Indicator Channel (PICH), the Dedicated Physical Channel (DPCH) and the HS-SCCHs are not transmitted. The power allocated to the active interfering channels is reassigned to the Orthogonal Channel Noise Simulator (OCNS) transmission, as suggested in [4]. The OCNS is described in further detail below. The HS-SCCHs are signalled error-free to the receiver, see Fig. 1.

Data streams for the HS-PDSCHs are generated randomly. The packet size is either defined by the signalled CQI and the UE capability class or by the testcases given in [5]. The information bits for each user are encoded according to [2]. The coding chain includes Cyclic Redundancy Check (CRC) attachment, channel coding (Turbo Coding), HARQ functionality, and interleaving.

All channels except for the SCH are modulated, spread by orthogonal Walsh-Hadamard sequences and subsequently scrambled by the cell-specific Gold sequence. All channels are then weighted and added to a single chip stream s_i according to [3]. The weighting factors are calculated from the relative power ratios of the channels to the total transmit power spectral density (E_c/I_{or}). To achieve a total transmit power spectral density of $I_{or} = 1$ ($0\,\mathrm{dB}$), further channels are generated by the OCNS and are added to the chip stream [5]. Those channels have a fixed spreading factor of $\mathrm{SF} = 128$ and are used to simulate the users or control signals on the other orthogonal channels of a downlink.

For correct implementation of the filtering operation induced by the downlink channel model, at least two consecutive subframes are generated at the HSDPA transmitter and buffered in RB1 (see Fig. 1). This approach is required for modelling the interference caused by the root raised cosine (RRC) filter at the transmitter, the delay spread of the channel, and the chip-matched filter (MF) at the receiver. After matched filtering the subframe is buffered in RB2 before it is read out by the receiver. The receiver processes the subframe including the spill-overs to adjacent subframes. In parallel, the code blocks of each subframe can be stored in RB3 for calculating the BER from the simulations if this is desired [6].

For throughput simulations only the information bits excluding CRC bits of acknowledged data blocks (CRC check does not fail) are summed up.

IV. Receiver Architecture

In this contribution, we evaluate the achievable throughput of the conventional RAKE receiver and an LMMSE equalizer. Equalization of the frequency selective radio channel may partially restore the orthogonality of downlink spreading sequences and mitigate MAI.

A. RAKE Receiver

The conventional RAKE receiver approximates a matched-filter for the channel's impulse response. Consequently, it first delays the received signal, then descrambles and despreads it, and finally performs combining with respect to the Maximum Ratio Combining (MRC) criterion. The coefficients are found through channel estimation, which is carried out using the P-CPICH. Specifically, we use a symbol-level least squares estimator computing the channel coefficients for each delay separately. The channel delays are assumed to be known at the receiver, since a path-searcher can be easily implemented in practice.

While this is a very simple and scalable scheme, it is not optimal in HSDPA since it does not take Multiple Access Interference (MAI) into account. This interference is caused by the multi-tap characteristics of the channel, which destroys the orthogonality between the users' spreading codes. Consequently, the CDMA codes can no longer be separated at the receiver, leading to significant performance degradation.

B. LMMSE Equalizer

Channel equalization is a broad topic and can be performed with respect to various criteria. In the scope of this paper we consider chip-rate LMMSE equalization, which is mathematically formulated as minimizing the cost-function

$$J(\mathbf{f}) = \mathbb{E}\left\{\left|\mathbf{f}^H\mathbf{r}_i - s_{i-\tau}\right|^2\right\} \ , \tag{1}$$

where $\mathbf{f}$ stands for the equalizer coefficients, $s_{i-\tau}$ is a delayed version of the transmitted chip stream and $\mathbf{r}_i$ is a column vector of the last L_f received (chip-spaced) samples.

A solution to (1) can be found in [11]

$$\mathbf{f} = \sigma_s^2 \left(\sigma_s^2\,\mathbf{H}\mathbf{H}^H + \sigma_v^2\mathbf{I}\right)^{-1}\mathbf{H}\mathbf{e}_\tau \ , \tag{2}$$

where

$$\mathbf{H} = \begin{bmatrix} h_0 & \cdots & h_{L_h-1} & & 0 \\ & \ddots & \ddots & \ddots & \\ 0 & & h_0 & \cdots & h_{L_h-1} \end{bmatrix} \tag{3}$$

stems from the convolution with the channel's impulse response $h[i]$, $\mathbf{I}$ stands for the identity matrix, and $\mathbf{e}_\tau$ is a unit vector with a one at the τ-th position. This corresponds to the delay induced by the filters and the channel. The matrix $\mathbf{H}$ has to be found through channel estimation, which is again performed with a symbol-level least squares estimator.

The LMMSE equalizer corrects for the distortion brought about by the channel and (partly) restores orthogonality. However, this is at the cost of making the receiver more complex since (2) shows that a $L_f \times L_f$ matrix inverse has to be computed.

Efficient implementations for the matrix inverse [12] are therefore desirable. Additionally, it is also possible to employ adaptive equalization, while almost retaining the performance of the LMMSE method [8].

C. Demodulation and Decoding

Upon equalization the UE descrambles, despreads and demodulates its assigned HS-PDSCH channels using the channelization sequences and modulation indices signalled in the HS-SCCH. The demodulator returns log-likelihood ratios (LLRs) of the bits. The LLR of a bipolar bit b is defined as

$$\ln\left(\frac{p(b=+1)}{p(b=-1)}\right), \tag{4}$$

where $p(\cdot)$ denotes probability and $\ln(\cdot)$ stands for the natural logarithm.

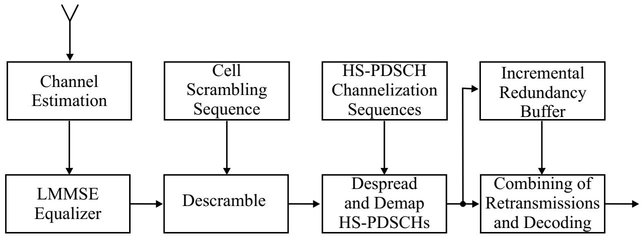

Fig. 2. HSDPA Receiver with LMMSE equalizer and IR Buffer

TABLE I
FIXED REFERENCE CHANNEL H-SET 3.

Parameter	Value	
Modulation	QPSK	16QAM
Nominal Avg. Inf. Bit Rate [kbps]	1601	2332
Inter-TTI Distance	1	1
No. of HARQ Processes	6	6
Coding Rate	0.67	0.61
No. of Physical Channel Codes	5	4

The LLR values are sent through an inverse rate matching block, which sets punctured bits to 0 and combines (i. e. adds up) repeated bits with bits previously stored in the IR buffer. The result is stored again in the IR buffer and sent to the Turbo decoder. The Turbo decoder uses the max-log-MAP algorithm with 8 iterations [13], [14].

V. NUMERICAL EXPERIMENTS

Throughput simulations for the just described HSDPA receiver with "UE Capability 6" [15] are carried out for QPSK and 16QAM. At the transmitter, the fixed reference channel H-Set 3, as defined in [5] is generated (see Table I).

The relative power ratios of the simulated physical channels to the total transmit power spectral density (E_c/I_{or}) are given in Table II and are set in compliance to the HSDPA test cases [5]. The E_c/I_{or} of the HS-PDSCH is varied.

No pathloss is assumed ($\hat{I}_{or} = I_{or}$) and the interference from other cells as well as the noise is modelled as AWGN

TABLE II
COMMON SIMULATION PARAMETERS.

Parameter	Value
UE Capability class	6
Max. No. of retransmissions	3
Combining	soft
RV coding sequence	$\{0,2,5,6\}$ for QPSK $\{6,2,1,5\}$ for 16QAM
P-CPICH E_c/I_{or}	$-10\,$dB
SCH E_c/I_{or}	$-12\,$dB
P-CCPCH E_c/I_{or}	$-12\,$dB
OCNS	on
$\hat{I}_{or}/I_{oc}$	$10\,$dB
Delay estimation	perfect
Channel coefficient estimation	least squares
Turbo decoding	max-log-MAP - 8 iterations
Oversampling factor	1

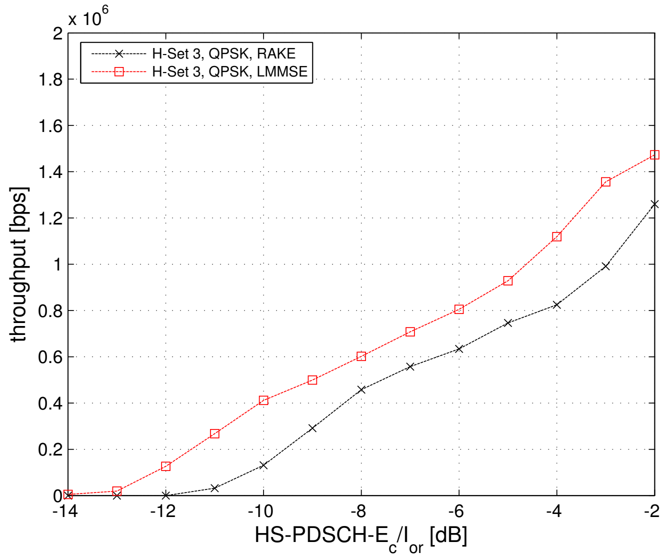

Fig. 3. QPSK throughput results for ITU PB3 channel for $\hat{I}_{or}/I_{oc} = 10\,\mathrm{dB}$.

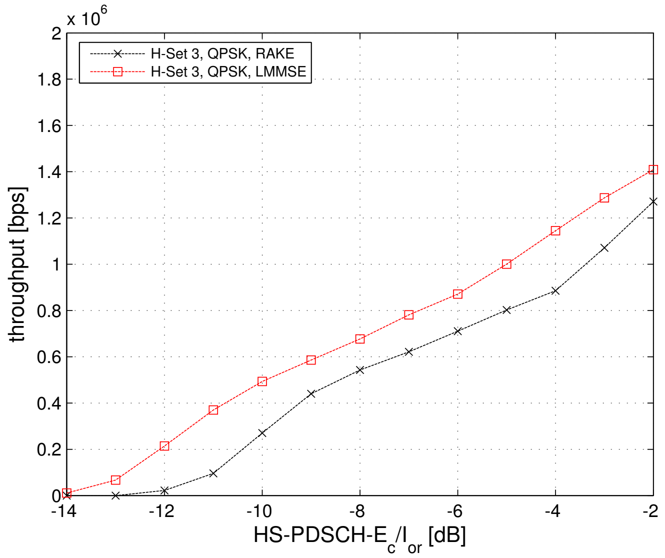

Fig. 4. QPSK throughput results for ITU VA30 channel for $\hat{I}_{or}/I_{oc} = 10\,\mathrm{dB}$.

with variance $\sigma^2 = I_{oc}$. We have used $\hat{I}_{or}/I_{oc} = 10\,\mathrm{dB}$ for QPSK and for 16QAM simulations.

Throughput simulations are carried out for two different frequency selective Rayleigh fading channels, namely ITU Pedestrian-B (PB3) and ITU Vehicular-A (VA30) [5]. These channel models define different power delay profiles with 6 paths at different delays. The mobile speed is $3\,\mathrm{km/h}$ for the PB3 channel and $30\,\mathrm{km/h}$ for the VA30. The L Rayleigh fading channel coefficients h_l are normalized to unit gain

$$\mathbb{E}\left(\sum_{l=1}^{L}|h_l|^2\right) = 1. \tag{5}$$

The received signal can be written as

$$r_i = \sum_{l=1}^{L} h_l s_{i-\tau_l} + n_i \tag{6}$$

where r is the received signal, s is the transmitted baseband signal and n is the i.i.d. zero-mean Gaussian noise with variance σ^2, and τ_l denote the delays in samples. For throughput simulations with RAKE receiver, the number of RAKE fingers is set to the number of propagation paths to collect the entire received energy. The results for QPSK are shown in Fig. 3 and Fig. 4 for PB3 and VA30. For 16QAM simulations Fig. 5 and Fig. 6 depict the throughput results for PB3 and VA30.

VI. Discussion of Results

The RAKE receiver front-end of a future HSDPA receiver suffers from a significant error floor due to interference from other channels which results in a degradation of the throughput. The LMMSE equalizer on the other hand corrects for the distortion brought about by the channel and (partly) restores orthogonality.

All simulation results show that the LMMSE equalizer has superior performance to the RAKE receiver. For the PB3 channel model and the QPSK reference channel (Fig. 3) the simulation results show a $1.8\,\mathrm{dB}$ performance gain of the LMMSE equalizer compared to the RAKE receiver. This results in a throughput enhancement of approx. 30% at an E_c/I_{or} of $-3\,\mathrm{dB}$. Furthermore at an E_c/I_{or} of $-1\,\mathrm{dB}$ nearly the maximum possible throughput is achieved. In the case of 16QAM the performance gain is approx. $2\,\mathrm{dB}$, Fig. 5. For the VA30 channel model, there is still a gain of approx. 1.6 dB for both QPSK and 16QAM (see Fig. 4 and 6).

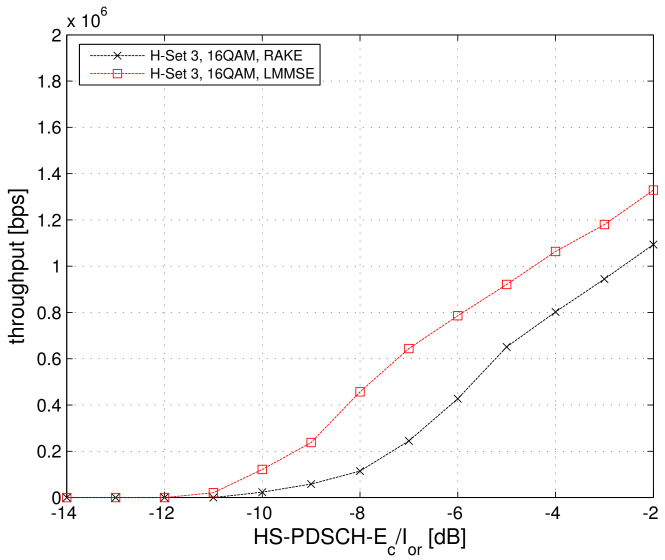

Fig. 5. 16QAM throughput results for ITU PB3 channel for $\hat{I}_{or}/I_{oc} = 10\,\mathrm{dB}$.

The minimum throughput requirements defined in [5] are just fulfilled with the RAKE easily outperformed with the LMMSE equalizer. This becomes important when implement-

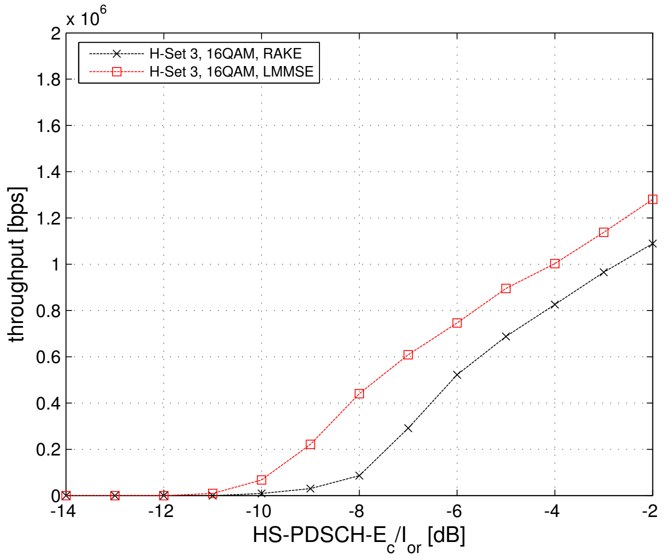

Fig. 6. 16QAM throughput results for ITU VA30 channel for $\hat{I}_{or}/I_{oc} = 10\,\mathrm{dB}$.

ing a HSDPA receiver in hardware because the expected implementation performance losses.

It is also worth noting that the throughput does not increase with the usage of 16QAM instead of QPSK for the simulated propagation channels. This confirms the fact that 16QAM was not intended for usage in channels with large delay spread.

VII. Conclusion

We have developed an HSDPA simulation environment for investigating potential mobile station receiver architectures. The downlink physical layer for the user data on the HS-PDSCH is modelled in detail, whereas the associated signalling is free of errors. The interference from signalling and data channels on the HS-PDSCH is modelled adequately.

Simulation results indicate that the Linear Minimum Mean Square Error (LMMSE) equalizer shows superior throughput than a conventional RAKE receiver. The gain in $E_{\mathrm{c}}/I_{\mathrm{or}}$ is approx. $1.6\,\mathrm{dB}$ for QPSK and $2\,\mathrm{dB}$ for 16QAM.

VIII. Acknowledgement

The authors would like to thank Markus Rupp for continuous encouragement and support. This work was partly funded by **K***plus*, Infineon Technologies, the ARC Seibersdorf Research GmbH (ARCS), and the University of Applied Science Hagenberg through the projects C3 and C9 at Forschungszentrum Telekommunikation Wien (ftw.).

References

[1] "Third Generation Partnership Project (3GPP)," http://www.3gpp.org/.

[2] Members of 3GPP, "Technical specification group radio access network; multiplexing and channel coding (FDD) (3GPP TS 25.212 version 6.1.0)," Mar. 2004.

[3] ——, "Technical specification group radio access network; spreading and modulation (FDD) (3GPP TS 25.213 version 6.0.0)," Dec. 2003.

[4] ——, "Technical specification group radio access network; high speed downlink packet access: UE radio transmission and reception (FDD) (3G TR 25.890 version 1.0.0)," May 2002.

[5] ——, "Technical specification group radio access network; User Equipment (UE) radio transmission and reception (FDD) (3GPP TS 25.101 version 6.4.0)," Mar. 2004.

[6] K. Freudenthaler, F. Kaltenberger, , S. Paul, C. F. Mecklenbräuker, M. Huemer, , and A. Springer, "Cancellation of interference from synchronization and pilot channels on high speed downlink shared channel in UMTS," in *Proc. of the 11th European Wireless Conference 2005*, Nicosia, Cyprus, Apr. 2005, pp. 498–503.

[7] F. Kaltenberger, K. Freudenthaler, S. Paul, J. Wehinger, C. F. Mecklenbräuker, and A. Springer, "Throughput enhancement by cancellation of synchronization and pilot channel for UMTS high speed downlink packet access," in *Proc. of the 6th International Workshop on Signal Processing Advances for Wireless Communications (SPAWC)*, New York City, USA, June 2005, to be published.

[8] S. Geirhofer, C. Mehlführer, and M. Rupp, "Design and real-time measurement of hsdpa equalizers," in *Proc. of the 6th International Workshop on Signal Processing Advances for Wireless Communications (SPAWC)*, New York City, USA, June 2005, to be published.

[9] M. Harteneck, M. Boloorian, S. Georgoulis, and R. Tanner, "Practical aspects of an HSDPA 14 Mbps terminal," in *Proc. of the 48th Annual Meeting of the International Society for the System Sciences (ASILOMAR)*, Pacific Grove, USA, July 2004, pp. 799–803.

[10] I. Forkel and H. Klenner, "High speed downlink packet access (HSDPA) - A means of increasing downlink capacity in WCDMA cellular networks?" in *Proc. of the 5th European Wireless Conference 2004*, Barcelona, Spain, Feb. 2004.

[11] P. Schniter and A. R. Margetts, "Adaptive Chip-Rate Equalization of Downlink Multirate Wideband CDMA," in *Proc. 36th Asilomar Conf. on Signals, Systems and Computers*, vol. 2, Nov. 2002, pp. 1228–1232.

[12] L. Mailaender, "Low-complexity implementation of CDMA downlink equalization," in *Proc. Second International Conf. on 3G Mobile Communication Technologies*, no. 477, Mar. 2001, pp. 396–400.

[13] G. Bauch and V. Franz, "A comparison of soft-in/soft-out algorithms for "turbo-detection"," in *Proc. of Int. Conf. on Telecommunications (ICT)*, Porto Carras, Greece, June 1998, pp. 259–262.

[14] M. Valenti and J. Sun, "The UMTS turbo code and an efficient decoder implementation suitable for software-defined radios," *International Journal of Wireless Information Networks*, vol. 8, no. 4, October 2001.

[15] Members of 3GPP, "Technical specification group radio access network; ue radio access capabilities definition (3GPP TS 25.306 version 6.3.0)," Mar. 2004.